

City Research Online

City, University of London Institutional Repository

Citation: Zhang, Y., Ye, Y., Wang, J., Tang, B. & Fu, F. (2025). Strength Prediction of Self-Compacting Concrete Using Improved RVM Machine Learning Method. International Journal of Concrete Structures and Materials, 19(1), 101. doi: 10.1186/s40069-025-00835-8

This is the published version of the paper.

This version of the publication may differ from the final published version.

Permanent repository link: https://openaccess.city.ac.uk/id/eprint/36173/

Link to published version: https://doi.org/10.1186/s40069-025-00835-8

Copyright: City Research Online aims to make research outputs of City, University of London available to a wider audience. Copyright and Moral Rights remain with the author(s) and/or copyright holders. URLs from City Research Online may be freely distributed and linked to.

Reuse: Copies of full items can be used for personal research or study, educational, or not-for-profit purposes without prior permission or charge. Provided that the authors, title and full bibliographic details are credited, a hyperlink and/or URL is given for the original metadata page and the content is not changed in any way.

City Research Online: http://openaccess.city.ac.uk/ publications@city.ac.uk/

RESEARCH Open Access



Strength Prediction of Self-Compacting Concrete Using Improved RVM Machine Learning Method

Yan Zhang^{1,3}, Yulong Ye^{1,3}, Junfeng Wang¹, Beichang Tang¹ and Feng Fu^{2,3*}

Abstract

Given the difficulty in determining the parameters of the compressive strength prediction model of self-compacting concrete and the low prediction accuracy, this study focuses on the applicability of the relevance vector machine (RVM) model constructed using various optimization techniques in predicting the strength of self-compacting concrete. The principal component analysis (PCA) is first used to reduce the dimension of the influencing factors. Then, the particle swarm optimization algorithm (PSO) is introduced into the RVM to establish a PCA–PSO–RVM collaborative optimization model, which is compared with the traditional regression model through various statistical indicators and error analysis. The results show that the collaborative optimization model prediction based on PCA–PSO–RVM performs outstandingly in all performance indicators. In the test set, the R² of the collaborative optimization model is 0.978, MAE is 0.123, MSE is 0.021, and RMSE is 0.150. The evaluation of quantitative indicators verifies that the collaborative optimization model is feasible and advanced in predicting the strength of self-compacting concrete. This study also provides a reference for the research on durability, rheological properties, and other material predictions of self-compacting concrete.

Keywords Machine learning, Relevance vector machine, Principal component analysis, Particle swarm optimization, Self-compacting concrete, Strength prediction

1 Introduction

In recent years, with the rapid development of the construction industry, concrete structures such as bridges, pile foundations, and high-rise buildings are constantly being used, and various projects have higher and higher requirements for the actual service life which is durability of concrete structures (Douglas,

Journal information: ISSN 1976- 0485 / eISSN 2234-1315.

*Correspondence:

Feng Fu

feng.fu.1@city.ac.uk; cenffu@yahoo.co.uk

¹ Guangxi Key Laboratory of Geomechanics and Geotechnical Engineering, Guilin University of Technology, Guilin 541004, China ² Department of Engineering, School of Science and Technology, City, University. of London, Northampton Square, London EC1V0HB, UK ³ College of Civil and Architectural Engineering, Guilin University

2019; Hooton & Bickley, 2014; Susilorini et al., 2022). However, the durability of concrete and construction quality are inseparable, especially the quality of concrete vibrating, which plays a key role in eliminating the phenomenon of honeycomb pitting of concrete, ensuring the quality of concrete components, and improving its strength and durability (Banfill et al., 2011; Koch et al., 2019; Zhang et al., 2021, 2024). At present, most of the concrete is manually pounded, as the concrete is not visible inside, the concrete pounding dense effect and quality control mainly depends on the experience of the construction personnel to judge, which leads to the uncertainty of the pounding quality and affects the durability of concrete (Tian et al., 2019). Self-compacting concrete (SCC) proposed by Japanese scholar Okamura in 1986 solves this problem well (Okamura & Ouchi, 1998). SCC does not need manual vibration, which



of Technology, Guilin 541004, China

© The Author(s) 2025. **Open Access** This article is licensed under a Creative Commons Attribution 4.0 International License, which permits use, sharing, adaptation, distribution and reproduction in any medium or format, as long as you give appropriate credit to the original author(s) and the source, provide a link to the Creative Commons licence, and indicate if changes were made. The images or other third party material in this article are included in the article's Creative Commons licence, unless indicated otherwise in a credit line to the material. If material is not included in the article's Creative Commons licence and your intended use is not permitted by statutory regulation or exceeds the permitted use, you will need to obtain permission directly from the copyright holder. To view a copy of this licence, visit http://creativecommons.org/licenses/by/4.0/.

avoids the original defects in concrete and can reduce the impact of construction quality on the durability of concrete structures. SCC relies on its own weight to pass through dense structural elements, fill the formwork, wrap reinforcement, and maintain stability and homogeneity, i.e., achieve full compaction and obtain optimal performance. By applying SCC in engineering, the construction period can be greatly shortened, labor costs, energy costs and equipment costs can be reduced, thereby improving economic efficiency.

Since the advent of SCC, it has been widely used in various engineering fields, such as construction and water conservancy. For example, it was used in railroads, high-rise buildings, dams, etc. (Zadeh et al., 2014; Zeng et al., 2021). The physical and mechanical properties of SCC, like ordinary pounded concrete, are the first to attract people's widespread attention. To obtain the best mix ratio for SCC strength, researchers have predicted SCC strength through rheological models, numerical methods, and experimental tests (Ding et al., 2018; Domone, 2007; Li et al., 2021) However, since SCC is composed of a mixture of multiple components, including high-cementitious materials and superplasticizers, each element has an impact on the mechanical properties of SCC. There is a strong coupling between the components, and the compressive strength and the components show a highly nonlinear mapping relationship (Siddique et al., 2011). Therefore, the above methods are still insufficient in describing the relationship between these mixed components and the compressive strength value of SCC. Determining its compressive strength has become an engineering problem that needs to be solved urgently (Rajakarunakaran et al., 2022).

With the development of artificial intelligence, many machine learning methods have been applied in civil engineering-related fields. Machine learning methods such as artificial neural networks, random forests, and support vector machines have been widely used in civil engineering (Akande et al., 2014; Asteris et al., 2024; Huang et al., 2019; Jahed et al., 2021; Mai et al., 2021; Skentou et al., 2023) Many scholars have established prediction models for the compressive strength of SCC based on machine learning. Dutta et al. (2017) predicted the compressive strength of SCC using three models: extreme learning machine (ELM) and multiple adaptive regression splines (MARS). However, these neural network models have their own imperfections, such as overfitting, poor ability to represent nonlinearity, and weak hermeneutics. Asteris P G (Asteris & Kolovos, 2019; Asteris et al., 2016) further used artificial neural networks to predict the strength of SCC, verifying the reliability of machine learning methods in predicting the strength of SCC. Tran V Q (Tran et al., 2022) predicted the compressive strength of SCC using the extreme gradient boosting (XGBoost) algorithm, and the accuracy was improved, but XGBoost still has the disadvantages of too many parameters, difficult to adjust the parameters, and long training time. Traditional models such as linear regression, decision tree, and support vector machine (SVM) have limitations in predicting the strength of SCC. They are not good enough in dealing with complex nonlinear patterns and may have overfitting problems in feature selection. Therefore, it is urgent to establish an efficient and reasonable model to accurately predict the compressive strength of SCC.

The relevance vector machine (RVM) is a highly sparse machine learning method proposed by Tipping (2001) based on the support vector machine which is based on Bayesian statistical theory and makes the model sparser by reducing the correlation vectors of the model. Moreover, the RVM algorithm provides posterior probability and the selection of kernel function is not restricted by Mercer conditions, which can continue to improve the model prediction ability on the basis of support vector machine. Kernel functions are functions used to map input data into a high-dimensional feature space. Able to handle more complex nonlinear problems. However, when the input sample influences (i.e., the number of sample dimensions) are large and there are coupling relationships and information redundancy among them, the learning efficiency of the RVM model will be reduced and the computational cost will be increased. At the same time, the generalization performance of RVM is sensitive to parameter settings. In general, the method of manual parameter adjustment is used to search for parameters, which is costly and is greatly affected by human factors. Using dimensionality reduction and optimization methods, the problem of RVM in SCC prediction can be well-solved. Principal component analysis (PCA) is one of the most commonly used methods for data analysis (Mrówczyńska et al., 2020). It can reduce the dimension of data, use fewer data dimensions, and retain more information about the original data, thereby improving the calculation speed of the model. The particle swarm algorithm has good optimization capabilities. Using the particle swarm algorithm (PSO) to find the optimal hyperparameters of the RVM model can improve the learning efficiency and generalization ability of the RVM model (Wu & Li, 2022).

This study organically combines principal component analysis, particle swarm optimization (PSO), and RVM to establish a PCA-PSO-RVM collaborative optimization model, develops an efficient and accurate SCC strength prediction model, and conducts a detailed analysis of the specific experimental data of 99 samples in the published literature (Saha et al., 2017). To verify the

superiority of the model, it is compared with 6 traditional regression models, including linear regression, multilayer perceptron regression (MLP), ridge regression, greedy algorithm (XGBoost) regression, random regression, and support vector machine regression (SVR). The collaborative optimization model not only improves the prediction accuracy and model generalization ability, but also promotes the intelligence of the SCC construction process, provides theoretical support and technical reference for the accurate prediction of concrete strength in engineering practice, and has important theoretical significance and engineering application value.

2 Fundamental

2.1 Principle of PCA

Principal component analysis (PCA) is one of the commonly used dimensionality reduction methods in data analysis (Yu et al., 2024), which uses orthogonal transformation to linearly transform multiple indicators with certain correlation in the original data and recombine them into a series of linearly uncorrelated variables. The information of the original variables is retained as completely as possible through fewer indicators to achieve the purpose of simplifying the data (Lee, 2021), the specific process is shown in Fig. 1.

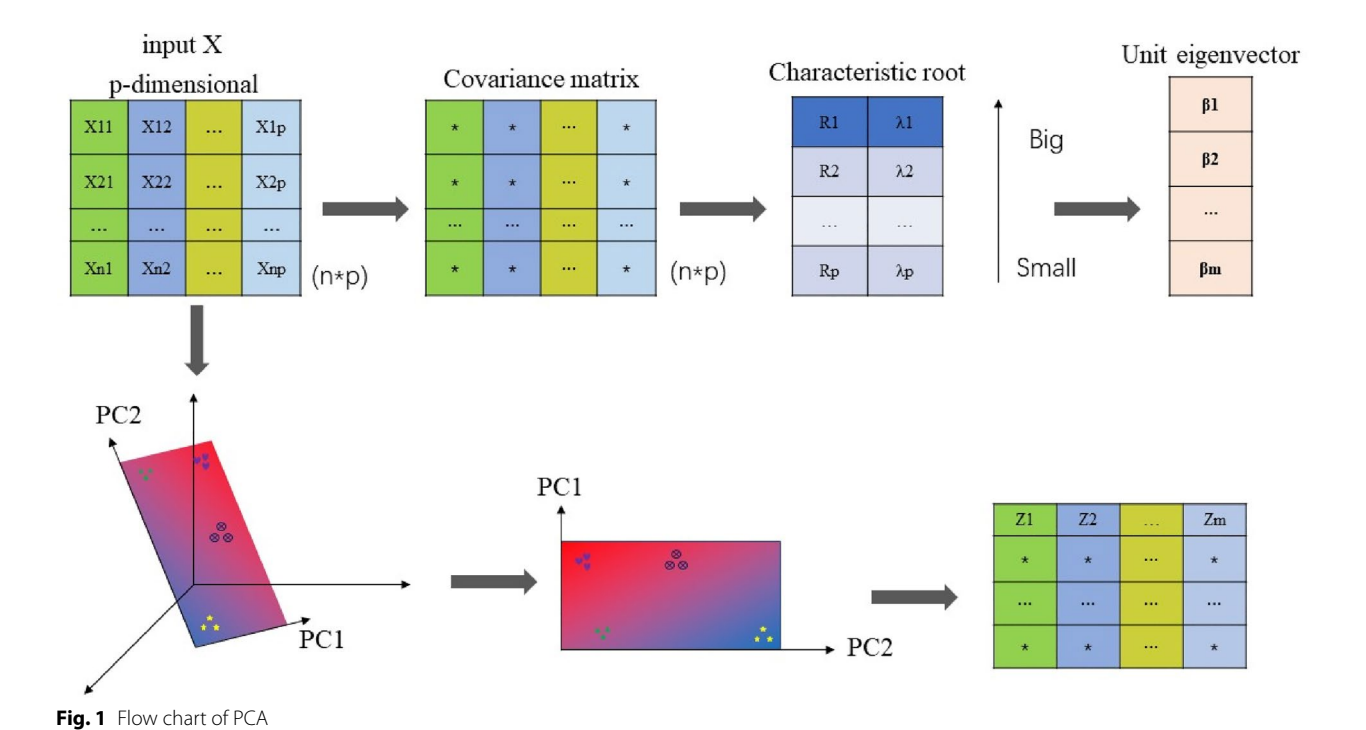
2.2 Principle of PSO

The PSO algorithm is an evolutionary algorithm developed by J. Kennedy and R. C. Eberhar through their research on the foraging behavior of bird flocks (Kennedy & Eberhart, 1995; Shami et al., 2022; Zoremsanga & Hussain, 2024). The algorithm is performed in an iterative recursive form, which has the advantages of high accuracy, fast convergence and less adjustment parameters required. It can be used to solve a large number of nonlinear, non-differentiable and multi-peak complex optimization problems (Gui et al., 2022). In PSO, each potential solution to an optimization problem is a particle in the search space. All particles have a fitness value determined by the optimization function, and each particle has a velocity that determines the direction and distance of their "flying", and then the particles follow the current optimal particle to search in the solution space, through the cooperation and competition in individuals to complete the search for optimal solutions in complex spaces, The PSO search process is shown in Fig. 2.

In finding the optimal value, the particle updates its velocity and position according to Eqs. (1) and (2) (Xing et al., 2022):

$$v_{id} = \omega v_{id} + c_1 r_1 (p_{id} - x_{id}) + c_2 r_2 (p_{gd} - x_{id})$$
 (1)

$$x_{id} = x_{id} + v_{id} \tag{2}$$



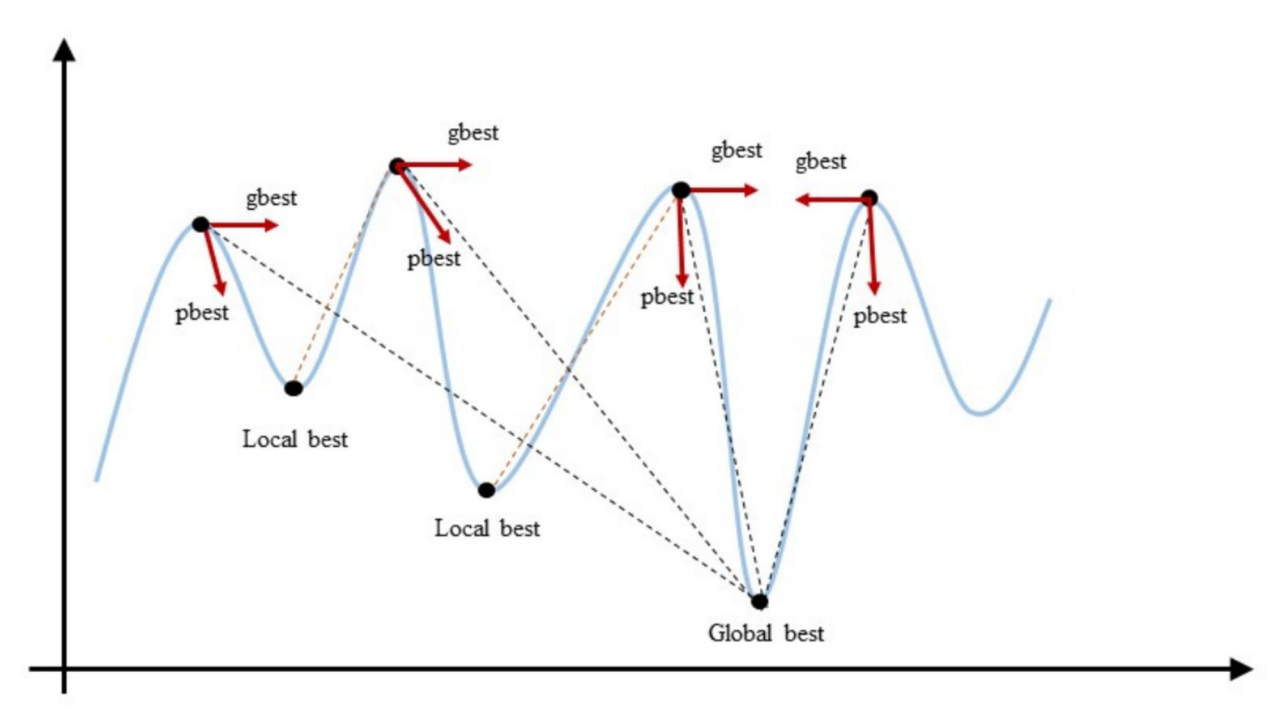


Fig. 2 Flow chart of PSO

where c_1 and c_2 are learning factors, r_1 and r_2 are uniform random numbers in the range of [0,1].

2.3 Principle of RVM

Relevance vector machine (RVM) transforms low-dimensional spatial nonlinear problems into high-dimensional spatial linear problems based on kernel function mapping. It has the following advantages: (1) few hyperparameters and high sparsity; (2) only the kernel parameters need to be set, which can save training time; and (3) the kernel function does not need to meet the Mercer condition, which greatly reduces the amount of calculation of the kernel function, the calculation process will be more efficient (Su et al., 2021; Wang et al., 2018).

First, given a training sample data set $\{x_n, t_n | n = 1, ..., 2, N\}$, x_n is the input value, t_n is the output target value. Assuming that t_n is independently distributed, the t_n function model is established as

$$t_n = \sum_{n=1}^{N} w_n K(x, x_n) + w_0 + \xi_n$$
 (3)

where $\omega_n - -$ Weight vector for mathematical model, $\omega = [\omega_0, \ \omega_1, \dots, \omega_n]^T$;

 $K(x,x_n)$ — — Kernel function of the model; ω_0 — — Indicates deviation;

 ξ_n — Represents the noise that follows the Gaussian distribution $(0, \sigma^2)$, this noise satisfies $\xi_n \sim N(0, \sigma^2)$;

$$\sigma^2$$
 — — Represents variance;

Assuming that t_n is distributed independently of each other, the likelihood function of the data set of training samples can be expressed as

$$p(t|\omega,\sigma^2) = (2\pi\sigma^2)^{-N/2} \exp\{-\frac{1}{2\sigma^2} \| t - \phi\omega \|^2\}$$
(4)

where $t = (t_1, t_2, ..., t_N)^T$; $\omega = [\omega_0, \omega_1, ..., \omega_n]^T$; $\Phi = [\varphi(x_1), \varphi(x_2), ..., \varphi(x_N)]^T$;

$$\varphi(x_n) = [1, K(x_n, x_1), K(x_n, x_2), \dots, K(x_n, x_N)]^T.$$

If the maximum likelihood approach is used directly to solve the problem, overfitting may occur in the process of using the RVM model. To avoid this phenomenon, the Bayesian perspective method is applied in the RVM model, and the size of each weight parameter ω_n is set to zero mean, which constitutes a basic distribution about ω that satisfies the Gaussian prior probability:

$$p(\omega|\alpha) = \prod_{n=0}^{N} N(\omega_n|0,\alpha_n^{-1})$$
 (5)

where $\alpha - - -$ represents the hyperparameter vector $\alpha = (\alpha_0, \alpha_1, \dots, \alpha_N)$

Among them, there is a corresponding relationship between the hyperparameter vector α and the weight

vector ω_i , and it will also directly determine the prior distribution of the weight vector ω_i . For each weight, the parameters in the above formula are independently distributed, which can greatly alleviate the complexity of the function distribution and realize the sparse characteristic of the RVM.

If the prior probability distribution of the RVM parameters is $P(\omega, \alpha, \sigma^2 | t)$, the posterior probability distribution of the training samples is as follows:

$$P(\omega, \alpha, \sigma^{2}|t) = \frac{P(t|\omega, \alpha, \sigma^{2})P(\omega, \alpha, \sigma^{2})}{P(t)}$$
(6)

Using Bayesian theory, the posterior distribution of the weight vector x can be expressed as follows:

$$P(\omega|t,\alpha,\sigma^2) = \frac{P(t|\omega,\sigma^2)P(\omega|\alpha)}{P(t|\alpha,\sigma^2)}$$
$$= (2\pi)^{-(N+1)/2} |\Sigma|^{-1/2} \exp\{-\frac{1}{2}(\omega-\mu)^T \Sigma^{-1}(\omega-\mu)\}$$

From the above, the probability distribution obeys a multivariate Gaussian model, $\Sigma = (\sigma^{-2}\phi^T\phi + A)^{-1}$ is variance, $\mu = \sigma^{-2}\Sigma\phi^Tt$ is mean value, $A = diag(\alpha_0, \alpha_1, \ldots, \alpha_N)$ is diagonal matrix. Since $P(\alpha, \sigma^2|t)$ cannot be calculated directly. Therefore, it is approximated by the Dirac Delta function, which is expressed as

$$P(\alpha, \sigma^2 | t) \approx \delta(\alpha_{MP}, \sigma_{MP}^2)$$
 (8)

After integrating ω in Eq. (7), the marginal distribution determined by the two parameters α and σ^2 can be obtained:

$$P(t|\alpha,\sigma^2) = \int P(t|\omega,\alpha)P(\omega|\alpha)d\omega \tag{9}$$

Then through maximum likelihood estimation and iterative calculation, the optimal solutions of parameters b and c are obtained:

$$\alpha_n^* = \frac{1 - \alpha_n \Sigma_{nn}}{\mu_n^2} \tag{10}$$

$$(\sigma^2)_n^* = \frac{\| \|t - \phi\mu\|^2}{N - \sum_{n=0}^{N} (1 - \alpha_n \Sigma_{nn})}$$
(11)

where Σii is the element corresponding to the ith diagonal in the covariance matrix Σ .

With the training sample data already given, the initial values of the parameters α and σ^2 are first assumed, and then the hyperparameters α and σ^2 are iterated through

Eqs. (10) and (11). In the iterative process, most α tends to infinity, and the corresponding ω tends to zero by applying the formula $\mu = \sigma^{-2} \Sigma \phi^T$. Thereby reducing the number of model basis functions, allowing the model to achieve a sparse effect, and the related parameters can converge faster to complete the training of the RVM model. The specific process is shown in Fig. 3.

In the process of using the RVM model algorithm, the selection of the kernel function will have an important impact on the training and prediction effects of the model. Compared with other kernel functions, the Gaussian kernel function has good processing ability for high-dimensional, low-dimensional, linear and nonlinear problems. Therefore, the Gaussian radial basis kernel function is selected as the kernel function of the RVM model in this research (Smola & Schölkopf, 2004). The Gaussian radial basis kernel function $K(x, x_i)$ can be expressed as

$$K(x, x_i) = \exp[-||x - x_i||/(2\sigma^2)]$$
 (12)

where σ^2 is the kernel function width.

2.4 Principle of PCA-PSO-RVM

Based on the above principles, the principle of PCA–PSO–RVM is shown in Fig. 4.

- 1. Normalization of the original data.
- 2. Using PCA to reduce the dimension of the influence features, a new data set was obtained after dimensionality reduction.
- 3. Initializing the PSO algorithm, using PSO to optimize the key parameters of the RVM model.
- 4. Train and predict the optimized model.
- 5. Compare the predicted value obtained by the optimal model with the actual value to analyze and verify the accuracy of the model. At the same time, the traditional machine learning model is used for comparative evaluation.

3 Data Processing and Model Building

3.1 Data Preprocessing and PCA Dimensionality Reduction to Determine Data Samples

Since the SCC itself has a lower water-cement ratio, higher sand rate, mixed with high-efficiency water reducing agents and high-cementitious materials, etc., in the composition of raw materials, ratio design methods are very different from ordinary concrete and general high-performance concrete, the original ordinary concrete work performance evaluation methods and principles are no longer applicable (Adhikary et al., 2022; Sabet et al., 2013). If all

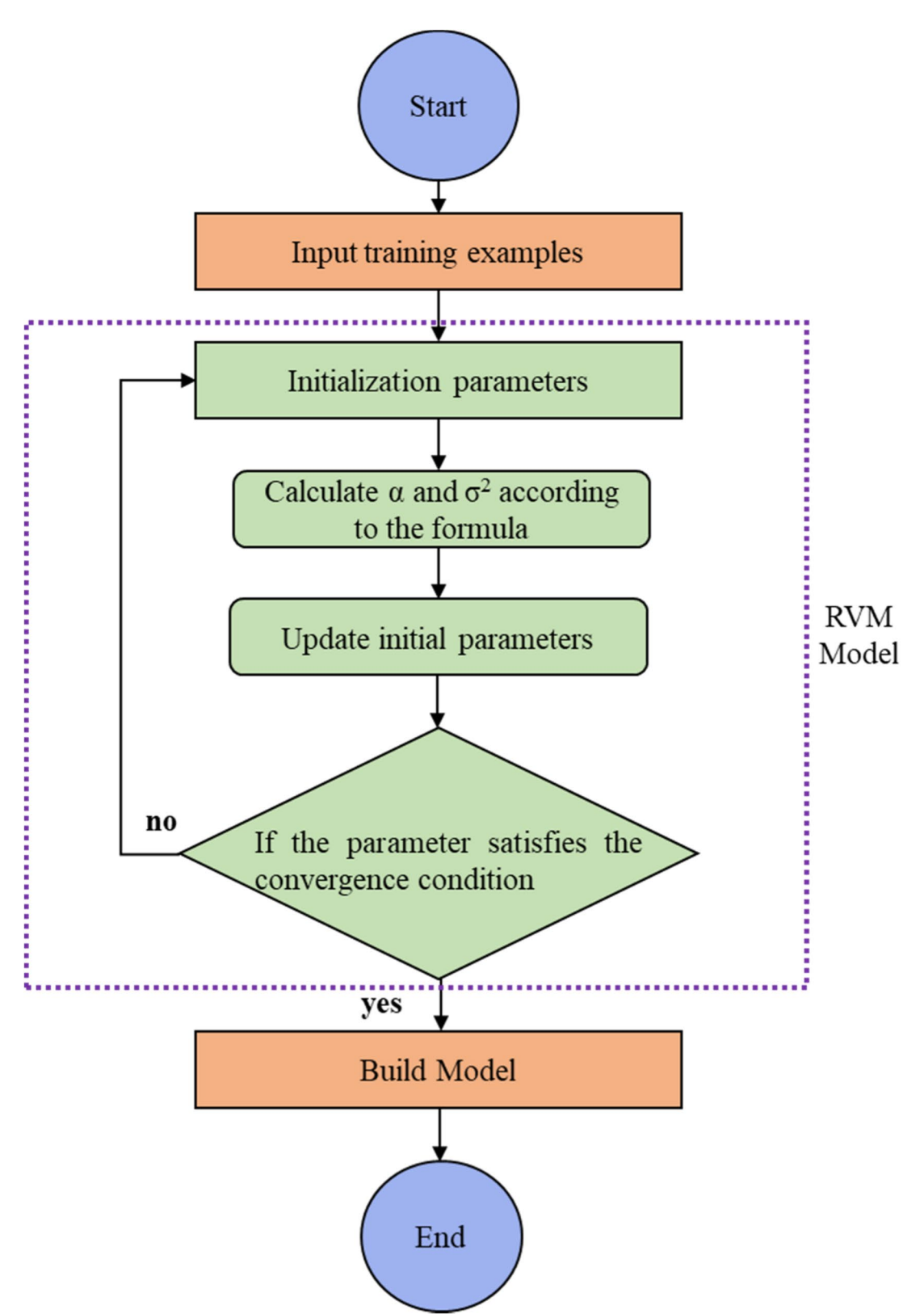


Fig. 3 Flow chart of RVM model training

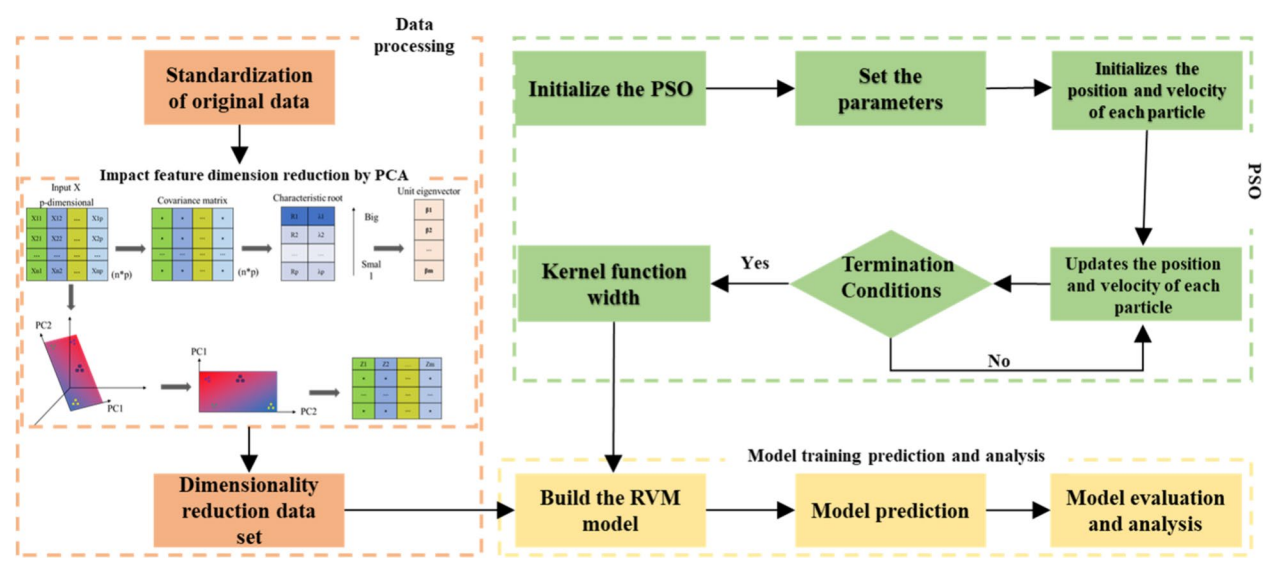


Fig. 4 Principle of PCA-PSO-RVM

influencing factors are used as input, the workload of the model will be increased, and the generalization and learning efficiency of the model will be reduced; however, if too few influencing factors are selected, the prediction accuracy of the model will be reduced. The relationship between each factor and the strength of SCC is now investigated using principal component analysis, analyze the main factors, and obtain new variables through dimensionality reduction. Then use the PSO optimization algorithm to optimize the key parameters of RVM, and use RVM to build a prediction model. Select 99 sets of data in the literature (Saha et al., 2017).

To reduce the impact of large magnitude differences between variables on correlation analysis, the 99 groups of data in Table 1 were standardized. The eigenvalues of the data were scaled between 0 and 1 to eliminate the magnitude differences between the eigenvalues, ensure the stability and effectiveness of the model training, and then perform a correlation analysis on eight indicators to obtain the correlation coefficient among the variables. Fig. 5 shows the heat map of the correlation coefficient between variables. Before conducting principal component analysis on the factors affecting the strength of SCC, Kaiser-Meyer-Olkin (KMO) test and Bartlett spherical test can be used to judge whether factor analysis is applicable among variables. If KMO \geq 0.5, sig≤0.5, it means that the factors affecting the strength of SCC can be analyzed by principal components. First, the KMO test was performed on the data, and the result was 0.5, indicating that there was a correlation between the variables, which met the requirements of factor analysis. The data were then subjected to Bartlett's sphericity test, and a significance p value of 0.000 was obtained, which is less than the significance level of 0.05 and presents significance at the level. The above test results show that the original sample data are suitable for factor analysis and the principal component analysis method can be used to reduce the dimension.

As can be seen from Fig. 5, the correlation coefficient values between the eight factors affecting the strength of SCC are all between -1 and 1. There is a correlation between the factors and a high degree of correlation between some of the indicators. To further explore the specific influence values of each factor, the score diagram of the influencing factors was obtained according to the PCA principle (Fig. 6).

The contribution rate and cumulative contribution rate of each factor were calculated for the 99 groups of 8 indicators after standardization (Table 2), and the visual graph is shown in Fig. 7. The contribution rate of the first principal component is 40%, the contribution rate of the second principal component is 20%, the contribution rate of the third principal component is 14%, and the contribution rate of the fourth principal component is 11%. The cumulative contribution rate of the first four principal components reaches 85%, and the contribution rates of the remaining factors can be ignored. In this way, the original 8 individual indicators are converted into 4 new mutually independent comprehensive indicators, and these 4 new comprehensive indicators represent 85% of the information of the original 8 individual indicators.

To further analyze the correlation between the principal components and the original indicators, a heat map of

 Table 1
 Self-compacting concrete strength data set

SI No	Cement (kg)	Ganister sand (kg)	Coarse aggregate(kg)	Fine aggregate(kg)	Poly propylene fiber (%)	Water (L)	Superplasticizer (L)	Viscosity- modifying admixture (L)	Compressive strength (MPa)
1	276	961	808	150	0	204	8.5	0.42	31.64
2	276	961	808	155	0.25	204	9.2	0.42	31.87
3	276	961	808	160	0.5	204	9.9	0.43	31.14
4	276	961	808	165	0.75	204	10.5	0.44	32.28
5	276	961	808	170	1	204	11.2	0.45	32.87
5	276	961	808	175	1.2	204	11.9	0.45	32.2
7	412	913	781	138	0	193	13.75	0.48	52.9
8	412	913	781	145	0.25	193	14.5	0.48	53.43
9	412	913	781	152	0.5	193	14.7	0.48	54.05
10	412	913	781	159	0.75	193	15.25	0.48	54.26
11	412	913	781	166	1	193	16	0.48	53.52
12	412	913	781	173	1.2	193	17.2	0.48	31.64
13	276	961	808	150	0	204	8.5	0.42	31.7
14	276	961	808	155	0.35	204	9.2	0.42	31.77
15	276	961	808	160	0.7	204	9.9	0.43	31.82
16	276	961	808	165	1.05	204	10.5	0.44	32.26
17	276	961	808	170	1.4	204	11.2	0.45	31.71
18	276	961	808	175	1.75	204	11.9	0.45	52.9
19	412	913	781	138	0	193	13.75	0.46	52.28
20	412	913	781	145	0.35	193	14.5	0.48	52.54
21	412	913	781	152	0.7	193	14.7	0.48	52.98
22	412	913	781	159	1.05	193	15.25	0.46	53.87
23	412	913	781	166	1.4	193	16	0.48	52.94
24	412	913	781	173	1.75	193	17.2	0.48	29.87
25	276	969	774	150	0	204	8.5	0.42	30.58
26	276	969	774	170	1.4	204	11.2	0.45	31.69
27	276	969	774	170	1	204	11.2	0.45	28.24
28	276	978	735	150	0	204	8.5	0.42	29.16
29	276	978	735	170	1.4	204	11.2	0.45	30.12
30	276	978	735	170	1	204	11.2	0.45	49.68
31	412	934	744	138	0	193	13.75	0.46	50.64
32	412	934	744	166	1.4	193	16	0.48	51.82
33	412	934	744	166	1	193	16	0.48	47.06
34	412	944	707	138	0	193	13.75	0.46	48.52
35	412	944	707	166	1.4	193	16	0.48	49.26
36	412	944	707	166	1	193	16	0.48	67.58
37	430	1050	715	100	0	185	5	0.6	65.19
38	430	1050	700	100	0	185	5	0.6	64.18
39	430	1100	690	100	0	185	5	0.6	68.53
40	430	1050	715	110	1	185	6	0.7	66.25
41	430	1050	700	110	1	185	6.7	0.7	65.38
42	430	1100	690	115	1	185	7	0.75	68.12
43	430	1050	715	110	1.4	185	6.5	0.7	65.61
44	430	1050	700	110	1.4	185	7	0.7	64.75
45	430	1100	690	120	1.4	185	, 7.5	0.75	37
46	340	920	815	75	0	190	7	0.5	34.9
47	340	920	800	75	0	190	7	0.5	32.5
48	340	950	795	75	0	190	7	0.5	32.5

 Table 1 (continued)

SI No	Cement (kg)	Ganister sand (kg)	Coarse aggregate(kg)	Fine aggregate(kg)	Poly propylene fiber (%)	Water (L)	Superplasticizer (L)	Viscosity- modifying admixture (L)	Compressive strength (MPa)
49	340	920	815	85	1	190	8	0.5	37.25
50	340	950	800	85	1	190	8	0.5	35.31
51	340	950	795	90	1	190	8	0.5	32.78
52	340	920	815	90	1.4	190	8	0.5	36.85
53	340	920	800	100	1.4	190	8.5	0.5	35.19
54	340	950	795	100	1.4	190	8.5	0.5	32.46
55	360	920	815	100	0	180	8	0.5	42
6	360	935	790	100	0	180	8	0.5	40.7
57	360	945	815	110	0	180	8	0.5	38.5
8	360	920	790	110	1	180	8.5	0.6	42.46
9	360	935	790	120	1	180	8.5	0.6	41.25
50	360	945	815	120	1	180	8.5	0.6	38.95
51	360	920	790	120	1.4	180	9	0.6	42.12
52	360	935	790	180	1.4	180	9	0.6	40.98
53	360	945	790	180	1.4	180	9	0.6	38.54
4	440	920	815	180	0	210	7	0.7	55
55	440	940	780	180	0	210	7	0.7	53.72
6	440	955	780	185	0	210	7	0.7	51.4
7	440	920	815	190	1	210	7.5	0.7	55.45
8	440	940	780	190	1	210	7.5	0.7	54.03
9	440	955	780	190	1	210	8	0.7	51.89
0	440	920	815	190	1.4	210	8	0.7	55.26
· 1	440	940	780	70	1.4	210	8.5	0.7	53.72
'2	440	955	780	70	1.4	210	8.5	0.7	51.69
'3	500	840	870	70	0	198	8.3	0.75	68
4	500	855	830	80	0	198	8.3	0.75	67
· '5	500	870	830	80	0	198	8.3	0.75	65.3
'6	500	840	870	85	1	198	9	0.75	68.5
7	500	855	830	85	1	198	9	0.75	67.67
' '8	500	870	830	85	1	198	9	0.75	65.1
'9	500	840	870	85	1.4	198	9	0.75	67.29
80	500	855	840	85	1.4	198	9	0.75	65
31	500	870	840	85	1.4	198	9	0.75	64.86
32	440	840	870	85	0	187	9	0.8	59
3	440	860	840	90	0	187	9	0.8	57.7
34	440	875	840	90	0	187	9	0.8	55.4
35	440	840	870	95	1	187	10	0.8	59.7
36	440	860	840	95	1	187	10	0.8	58.51
7	440	875	840	95	1	187	10	0.8	55.96
8	440	840		95					59.41
8 9	440	860	870	95 95	1.4	187	10	0.8	58.26
0	440	875	840	95 95	1.4	187 187	10	0.8	58.26 55.67
			840		1.4	187	10	0.8	
)1)2	460	840	870	70 70	0	183	9.2	0.9	63
	460	865	850	70	0	183	9.2	0.9	60.9
13	460	880	850	70	0	183	9.2	0.9	58.9
4	460	840	870	80	1	183	9.7	0.9	63.6
15 16	460	865 880	850 850	80 80	1	183 183	9.7 9.7	0.9 0.9	61.45 64.48

Table 1 (continued)

SI No	Cement (kg)	Ganister sand (kg)	Coarse aggregate(kg)	Fine aggregate(kg)	Poly propylene fiber (%)	Water (L)	Superplasticizer (L)	Viscosity- modifying admixture (L)	Compressive strength (MPa)
97	460	840	870	80	1.4	183	9.7	0.9	63.27
98	460	865	850	80	1.4	183	9.7	0.9	61.29
99	460	880	850	80	1.4	183	9.7	0.9	64.13

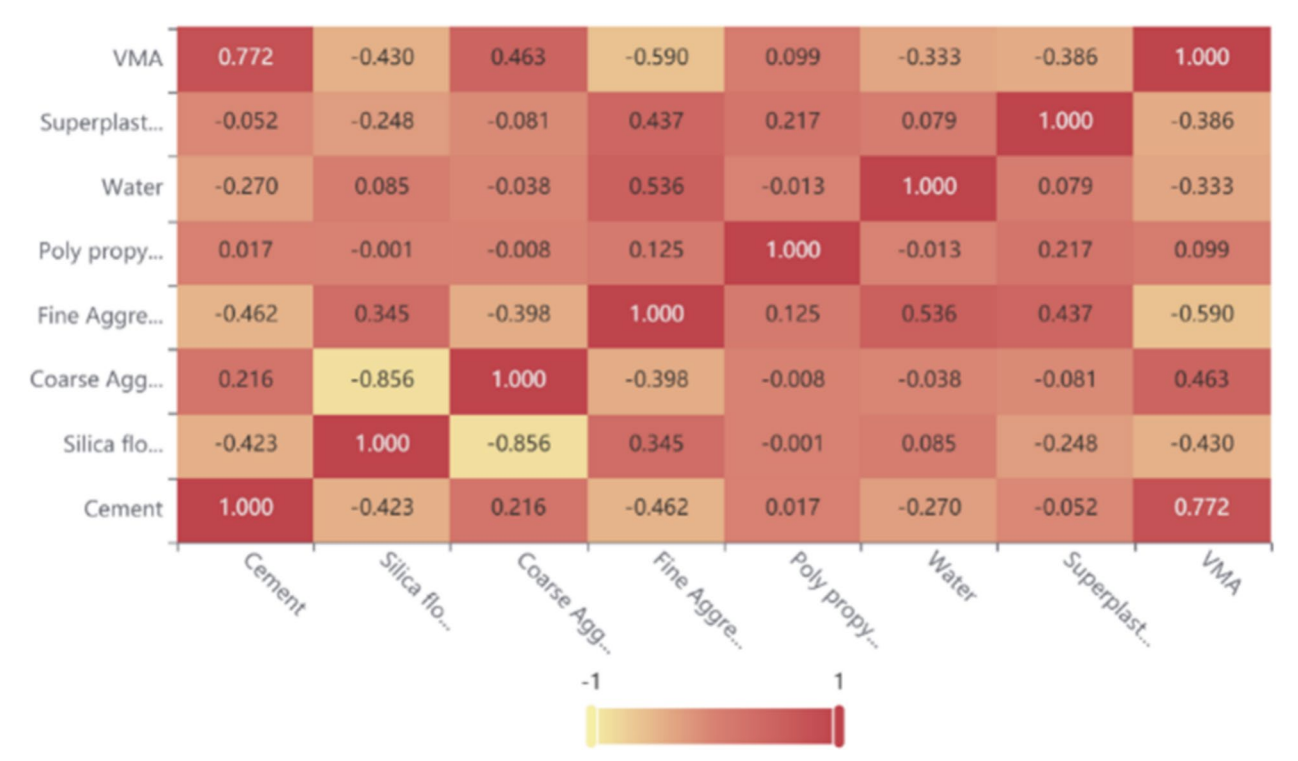


Fig. 5 Heat map of correlation coefficient

the factor loading matrix of the principal components is drawn (Fig. 8), from which the importance of the hidden variables in each principal component can be analyzed. The depth of the color in Fig. 8 represents the importance of the original influencing factors in the principal components, and the lighter the color, the higher the importance.

Through the analysis of Table 2 and Fig. 8, the importance of hidden variables in each principal component can be obtained.

For example, the first principal component (PC1) has an eigenvalue of 3.23, accounting for 40% of the total variance, indicating that cement, coarse aggregate, and viscosity-modifying admixture are the key factors influencing concrete strength. Cement (loading coefficient 0.738), as the primary binding material, directly determines strength through its hydration reactions. Coarse aggregate (0.688) serves as the skeletal framework, with

its strength and interfacial bonding significantly affecting load-bearing capacity. The viscosity-modifying admixture (0.874) substantially enhances compactness and strength by optimizing workability and microstructure (e.g., reducing porosity and improving the interfacial transition zone). The synergistic effects of these three components make them the main drivers of strength variation, reflecting the fundamental influence of material composition and processing technology on mechanical performance.

The second principal component (PC2) exhibits an eigenvalue of 1.60, accounting for 20% of the total variance, indicating its secondary importance relative to PC1. The corresponding eigenvector analysis reveals that the superplasticizer (loading coefficient 0.726) is the dominant influencing factor. This observation can be attributed to the superplasticizer's remarkable ability to enhance cement particle dispersion through combined

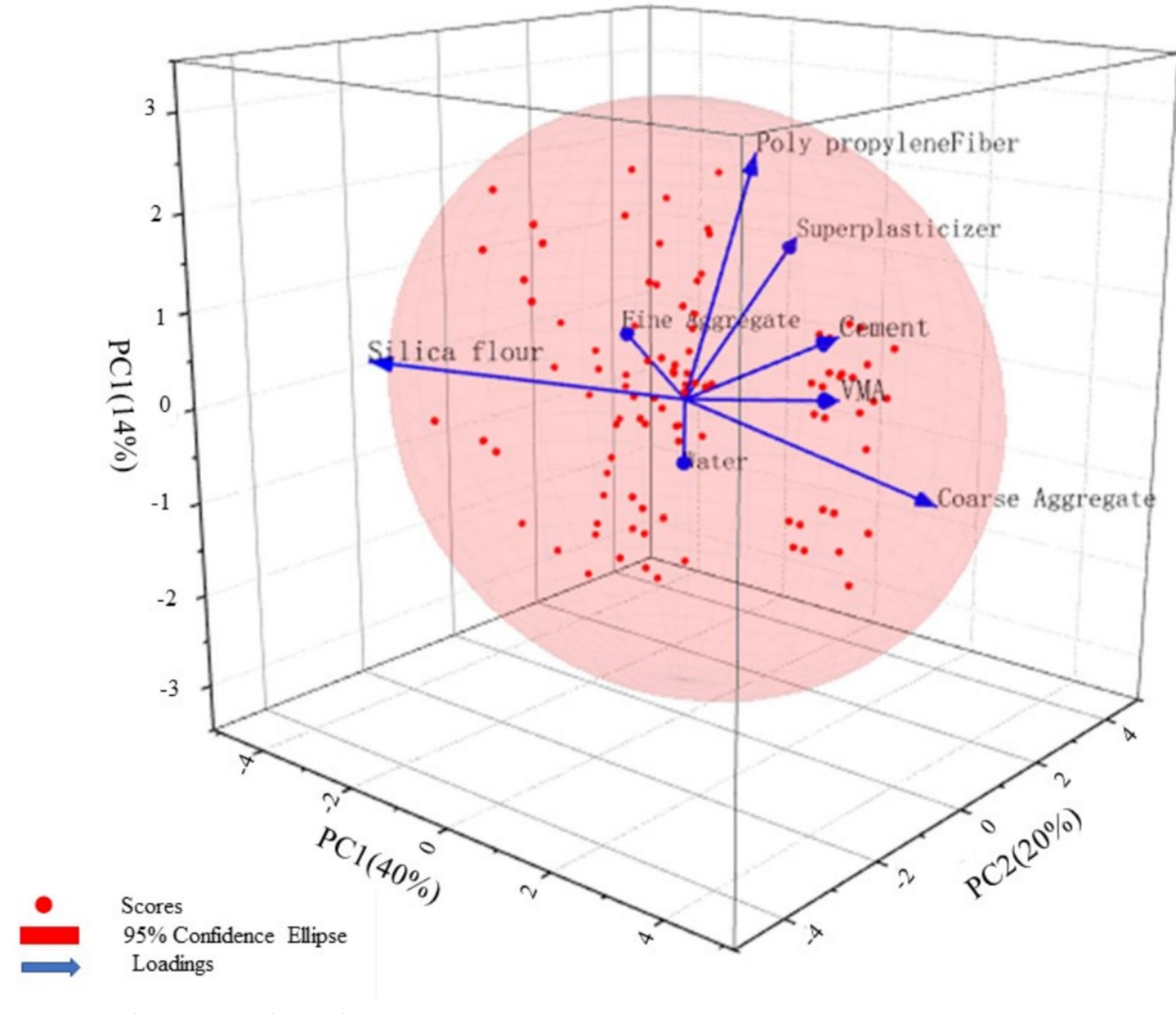


Fig. 6 Principal component analysis results

electrostatic repulsion and steric hindrance effects. At equivalent workability requirements, this mechanism enables significant water-to-cement ratio reduction,

Table 2 Table of cumulative contribution of each component

Principal components	Feature root	Contribution	Cumulative contribution
1	3.23	0.40	0.40
2	1.60	0.20	0.60
3	1.16	0.14	0.74
4	0.89	0.11	0.85
5	0.77	0.10	0.95
6	0.28	0.04	0.98
7	0.10	0.01	0.99
8	0.04	0.01	1.00

thereby substantially improving concrete compactness and long-term strength development. The 20% contribution rate demonstrates that while the strength-enhancing effect of superplasticizers is considerable, it remains secondary to the cementitious system (PC1, 40%). This finding aligns with the fundamental principle in concrete materials science that "cementitious materials dominate while water reducers optimize" the overall performance.

The third principal component (PC3) demonstrates an eigenvalue of 1.16, contributing 14% of the total variance. The eigenvector analysis identifies polypropylene fibers as the predominant influencing factor, with a correlation coefficient of 0.736. These fibers primarily function through a three-dimensional network structure that effectively inhibits microcrack propagation. Their bridging effect can enhance flexural strength by 15–25%, yet their overall contribution

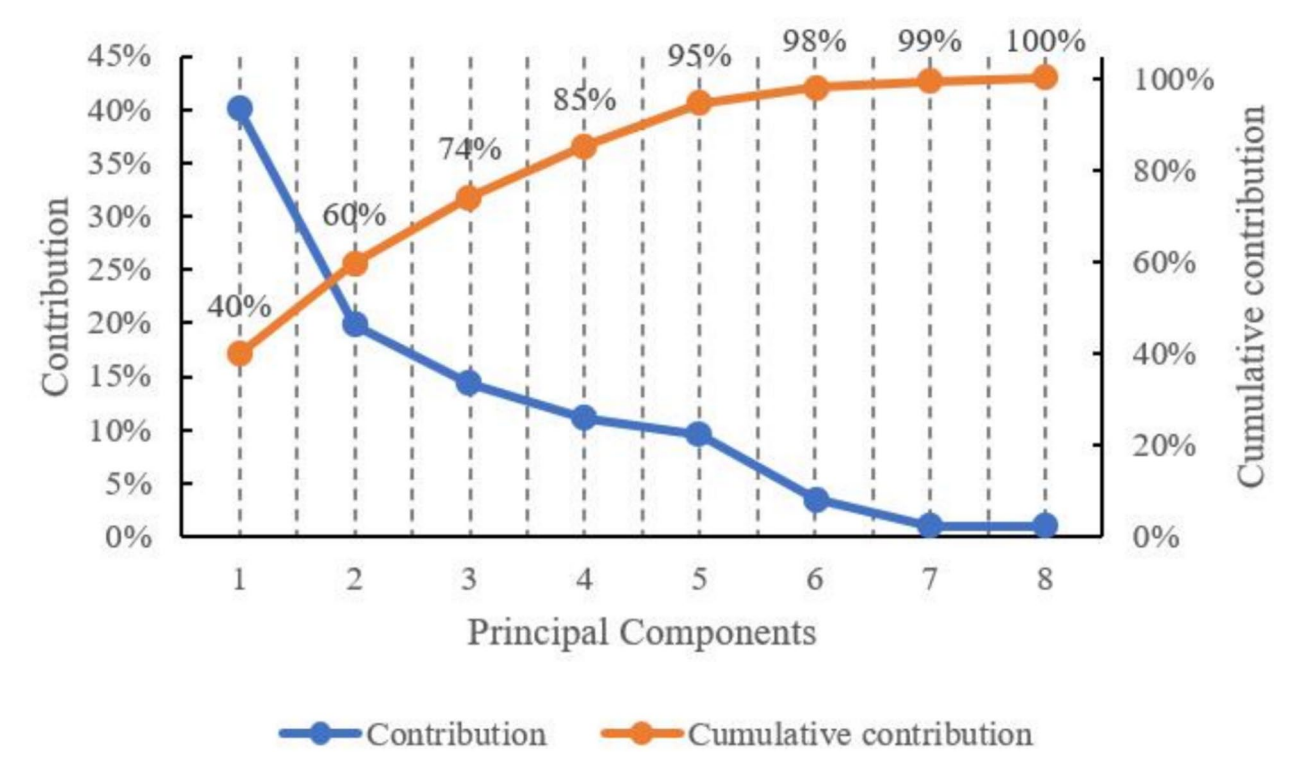


Fig. 7 Cumulative contribution of each component

VMA	0.874	-0.129	0.161	0.301	0.161	0.189	0.199	-0.044	1
Superplasticizer	-0.296	0.726	0.351	-0.438	0.204	-0.089	0.139	0.036	1
Water	-0.466	0.366	-0.419	0.592	0.264	-0.224	0.049	-0.005	1
Poly propyleneFiber	-0.029	0.309	0.736	0.441	-0.4	-0.072	-0.043	-0.003	1
Fine Aggregate	-0.797	0.355	0.044	0.157	0.207	0.407	-0.064	-0.004	1
Silica flour	0.688	0.495	-0.391	0.074	-0.307	0.109	0.002	0.132	1
Coarse Aggregate	-0.69	-0.665	0.19	0.132	0.023	0.009	0.09	0.138	1
Cement	0.738	-0.013	0.305	0.084	0.573	-0.057	-0.138	0.066	1
	PC1	PC2	PC3	PC4	PC5	PC6	PC7	PC8	Commonality

Fig. 8 Heat map of the factor load matrix

to compressive strength is constrained by three critical factors: first, the fiber reinforcement mechanism is dependent on matrix properties, representing a secondary strengthening effect. Second, the optimal dosage range is remarkably narrow (0.6–1.2kg/m³), with excessive amounts potentially inducing adverse effects. Finally, fibers predominantly modify mortar-phase performance while exhibiting limited influence on the interfacial transition zone of coarse aggregates. These inherent characteristics result in a contribution rate

that is inherently lower than both the cementitious system (PC1, 40%) and the superplasticizer system (PC2, 20%), consistent with established principles in fiber-reinforced concrete technology.

The fourth principal component (PC4) exhibits an eigenvalue of 0.89, accounting for 11% of the total variance. The corresponding eigenvector analysis identifies water content (correlation coefficient: 0.592) as the predominant influencing factor. The relatively lower ranking of water's impact on concrete strength

(fourth position) can be systematically explained through three key aspects: first, modern concrete mix design methodologies predominantly employ high-range water reducers (the primary indicator in PC2) for precise water—cement ratio control, which substantially diminishes the independent influence of water content. Second, water's functional mechanism has been partially incorporated within the cementitious system (the dominant indicator in PC1) through hydration processes. Third, water's influence on strength development demonstrates pronounced nonlinear characteristics, with its effects becoming significantly noticeable only when the water—cement ratio deviates from the optimal range. These analytical

findings demonstrate excellent consistency with the fundamental principles of water–cement ratio theory in concrete materials science.

3.2 Building a Prediction Model

In this study, four principal components after dimension reduction by principal component analysis are selected as input values, and the actual strength of SCC is used as output values. Among them, 70 groups were randomly selected as training group data, and the remaining 29 groups were used as test group data. The PSO algorithm is used to find the optimal parameters of the RVM model, and the collaborative optimization model is used to predict the predicted value, which is compared with the

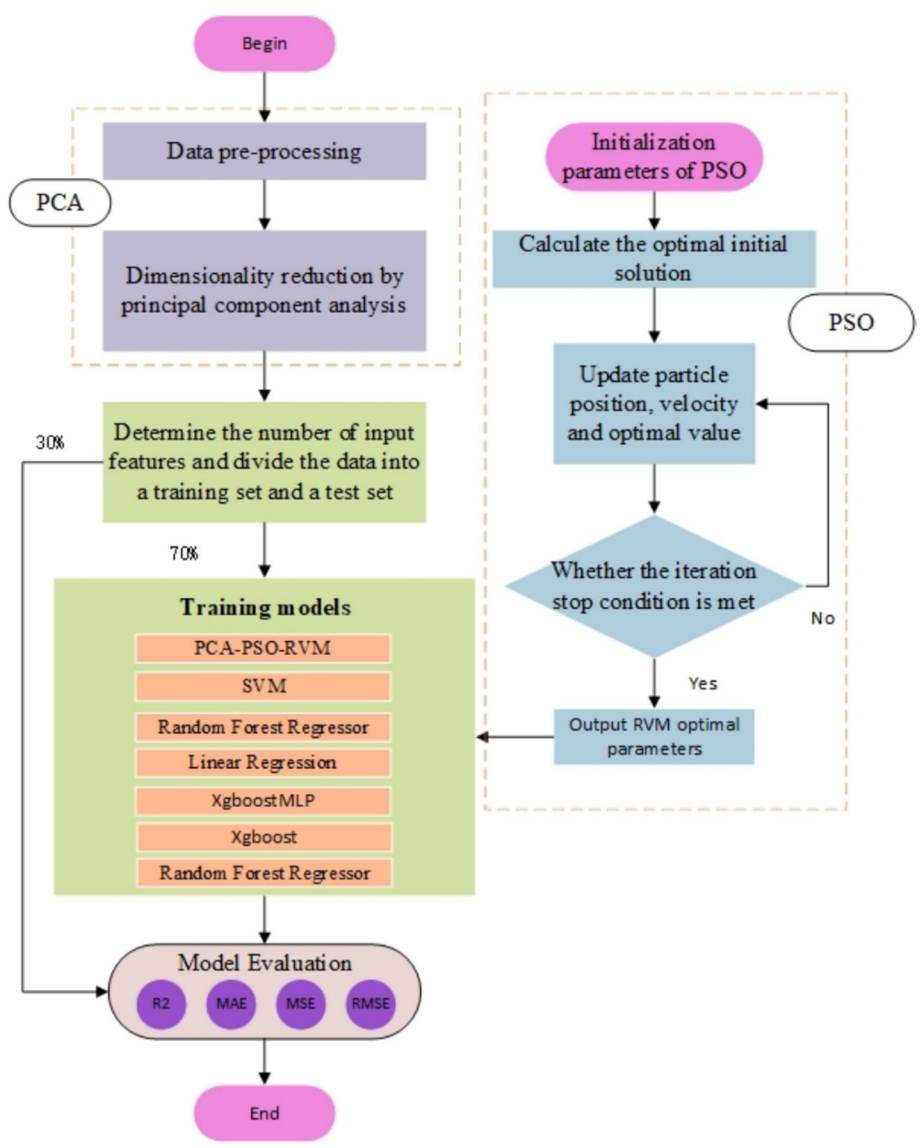


Fig. 9 Self-compacting concrete strength prediction model based on PCA-PSO-RVM

actual value to evaluate the accuracy of the model. The strength prediction model of SCC based on PCA-PSO-RVM is shown in Fig. 9.

The specific steps of modeling the SCC strength prediction model based on PCA-PSO-RVM are as follows:

- 1. The data are standardized first, and then the principal component analysis method is used to reduce the dimensionality of the 8 influencing factors to 4, which can retain 85% of the information of the original data.
- The PSO algorithm is used to optimize the parameters of the RVM model, and after finding the hyperparameters that meet the accuracy requirements, the hyperparameters of the RVM model are initialized.
- The PCA-PSO-RVM prediction model is established, and the standardized data are divided into training set and test set, which are used for model training and model prediction effect detection respectively.
- 4. Model evaluation, through the evaluation and analysis of multiple indicators of the sample measured value and the corresponding predicted value, and compared with other traditional regression models, to verify the accuracy of the established RVM prediction model.

3.3 Parameter Selection

The Gaussian kernel width has a great influence on the accuracy of the model. If the value is too small, it will easily lead to overfitting of the model, and the deviation of the test set will be large. If the value is large, it will easily lead to underfitting of the model, and the accuracy of the model will be low. In this study, the PSO algorithm is utilized to optimize the Gaussian kernel width to determine the optimal kernel width and ensure the reliability of the model. The number of particles is set (usually 20), the maximum number of iterations Tmax is set to 100-200, the inertia weight w is usually initialized to 0.9, the learning factor is set to 2.0, and the number of particles is set to 20. After optimization by the PSO algorithm, the optimal Gaussian kernel width for the RVM (Relevance Vector Machine) is found to be 0.653. By observing the iteration curve, the process is stopped when the curve becomes stable. As shown in Fig. 10, the curve tends to stabilize at the 52nd iteration, indicating that the particle swarm may have approached the optimal solution region. However, stopping too early (such as directly choosing 52 iterations) may lead to incomplete convergence of the algorithm. By extending the iterations to 100 times, premature convergence can be avoided. If the number of iterations exceeds 100, it will increase the computational time, and the performance improvement may be minimal. Therefore, in this paper, the number

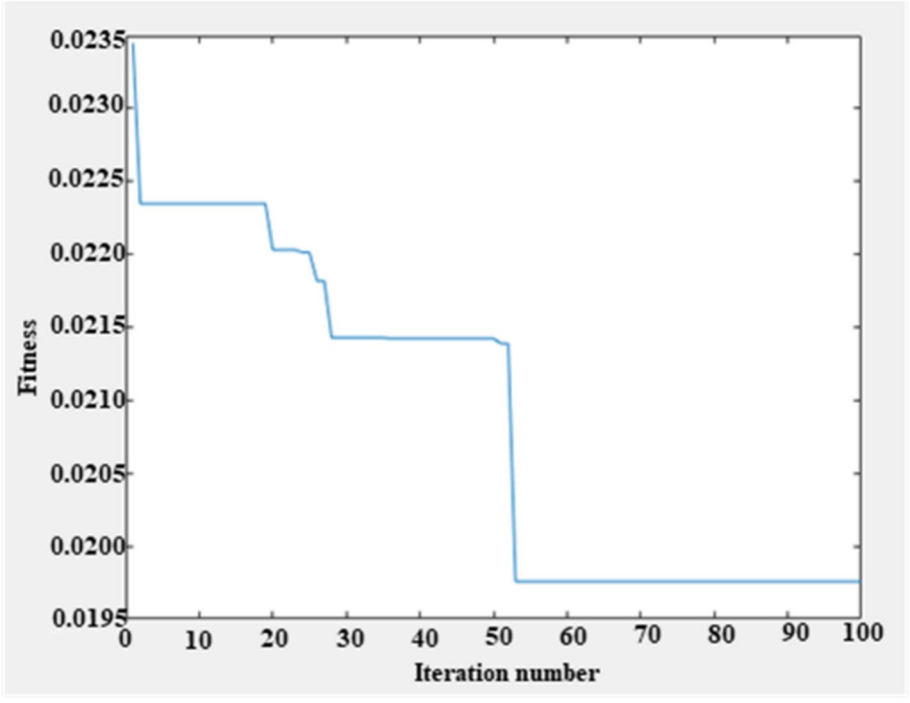


Fig. 10 Iteration curve graph

of iterations is chosen to be 100, at which the model results are optimal.

4 Prediction Result Analysis and Comparison with Other Models

4.1 Analysis of Examples

In this study, the proposed PCA-PSO-RVM model is employed to analyze and predict engineering case studies. The model is trained and optimized using the training data set, and its predictive performance is subsequently evaluated using the test data set. The prediction results are shown in Fig. 11. The specific values are shown in Appendix A. As can be seen from Fig. 11, the PCA-RVM model can accurately calculate the strength of SCC in the test data set, to obtain the degree of fitting between the predicted results and the measured results, a linear fit is performed between the predicted and measured values,

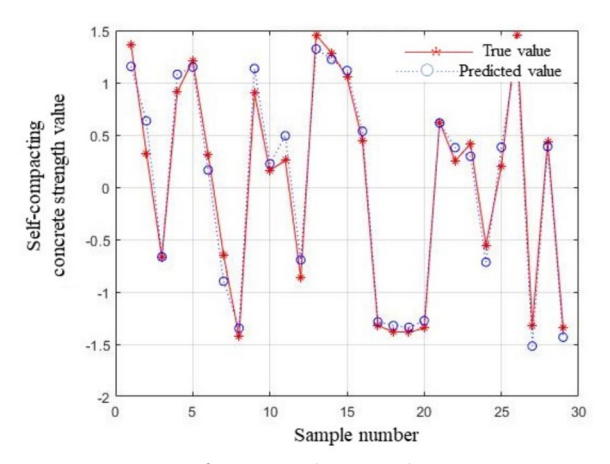


Fig. 11 Comparison of test set prediction results

as shown in Fig. 12. As can be seen in Fig. 11, the PCA–PSO–RVM regression model can fit the actual situation accurately, and the difference between the model predicted and actual values is small.

4.2 Evaluation Model

To verify the validity and superiority of the PCA–PSO–RVM model in the strength prediction of SCC, the linear regression (LR), the multilayer perceptron regression (MLP), the ridge regression (RR), the XGBoost regression, random forest regressor (RF), and support vector machine regression (SVR) to compare the prediction results.

To quantify the quality of the computational model and evaluate the performance of the model more reasonably, this study uses the coefficient of determination (R^2) , mean absolute error (MAE), mean square error (MSE), and root mean square error (RMSE) as four indicators to evaluate the model. The a_{20} index is further used to conduct reliability analysis and control of the model performance. Among them, MAE measures the average difference between the predicted value and the actual value, reflecting the actual situation of the forecast error; MSE reflects a measure of the degree of difference between the estimator and the estimated value; RMSE reflects the accuracy of the forecast; R2 reflects the goodness of fit of the model. The larger the value, the closer the predicted value is to the actual value. a_{20} is the percentage of samples whose deviation between the predicted value and the actual value is within ±20%. The closer the value is to 1, the better the model performance. The calculation formulas of each indicator are shown

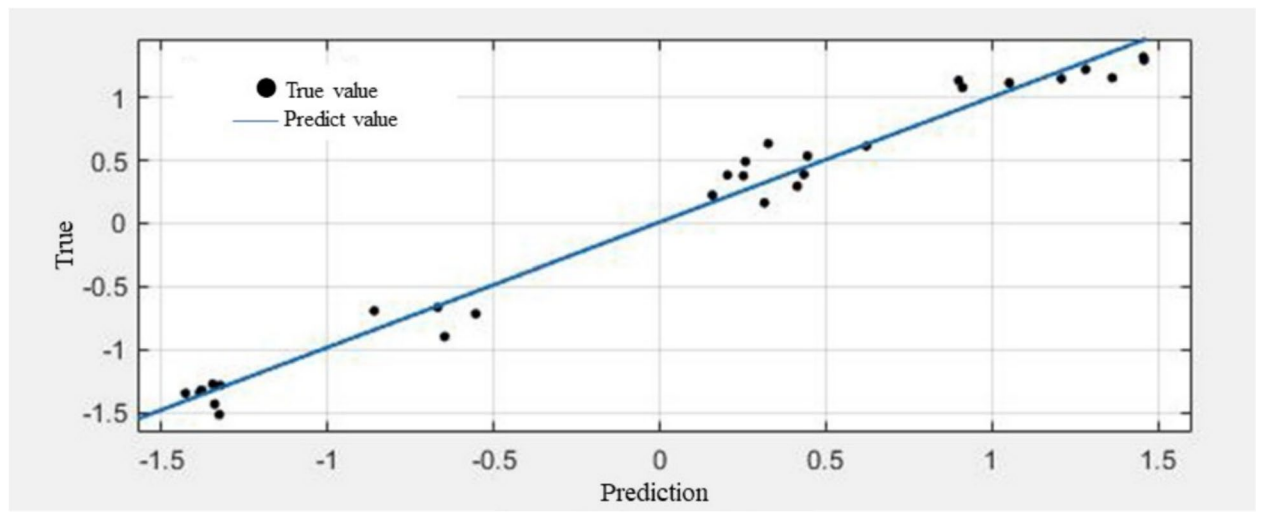


Fig. 12 Test set regression fit graph

in formula. (18–22) (Apostolopoulou et al., 2020; Armaghani and Asteris, 2021):

$$R^{2} = 1 - \frac{\sum_{i=1}^{n} (y_{i} - \hat{y_{i}})^{2}}{\sum_{i=1}^{n} (y_{i} - \bar{y_{i}})^{2}}$$
(13)

$$MAE = \frac{1}{n} \sum_{i=1}^{n} |y_i - \hat{y}_i|$$
 (14)

$$MSE = \frac{1}{n} \sum_{i=1}^{n} (y_i - \hat{y_i})^2$$
 (15)

$$RMSE = \sqrt{\frac{1}{n} \sum_{i=1}^{n} (y_i - \hat{y_i})^2}$$
 (16)

$$a_{20} = \frac{m_{20}}{M} \tag{17}$$

where y_i is the actual value; \hat{y}_i is the predicted value; \bar{y}_i is the average of the actual values; m_{20} is the number of samples for which the ratio of "actual value" to "predicted value" is between 0.80 and 1.20; M is the total number of samples in the data set.

The prediction evaluation indicators of each model can be obtained as shown in Table 3. To represent the prediction results of each model more clearly, the plots of the models under each evaluation index are drawn (Figs. 13, 14).

It can be seen from Table 3, Figs. 13 and 14 that the coefficient of determination R² of the PCA-PSO-RVM model is the closest to 1, which is 0.978, followed by SVR, which is 0.930; the MAE of the PCA-PSO-RVM model is closest to 0, followed by SVR. The MSE and RMSE of each model are the same as the distribution results of MAE, i.e., PCA-PSO-RVM is optimal among all models. Statistical studies on coefficient of

Table 3 Table of prediction accuracy of each model

Model	RMSE	MSE	MAE	R ²
PCA-LR	0.626	0.391	0.544	0.418
PCA-MLP	0.349	0.122	0.263	0.833
PCA-RR	0.626	0.392	0.544	0.408
PCA-XGboost	0.368	0.135	0.300	0.802
PCA-RF	0.350	0.122	0.284	0.833
PCA-SVR	0.227	0.052	0.179	0.930
PCA-PSO-RVM	0.150	0.021	0.123	0.978

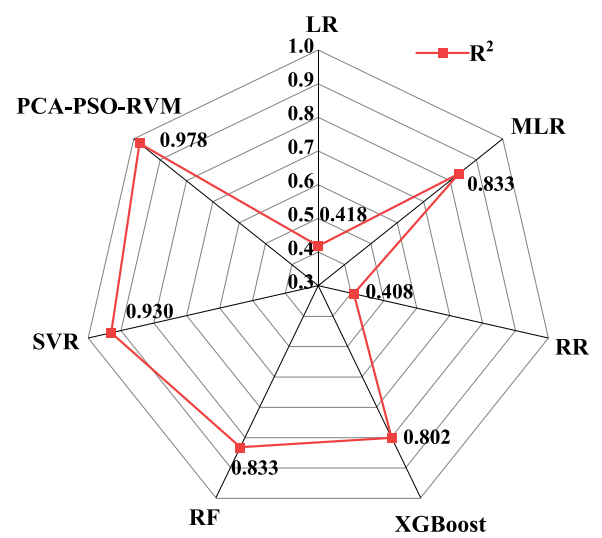


Fig. 13 R² evaluation indicators for each model

determination R², MAE, MSE, and RMSE show that the PCA-PSO-RVM model has the best robustness and is more accurate than other models in all aspects.

4.3 Performance Evaluation

Linear regression was used as the baseline model for the prediction of SCC strength. The linear regression model has a high error index. Although it can discover the linear trend between the strength of SCC and the influencing characteristics, it performs poorly in complex nonlinear relationships. In contrast, other models have a significant performance improvement. They show significant advantages in representing nonlinear relationships. However, these models often show a tendency to overfit when dealing with a small amount of training data or high-dimensional data, and there is still room for improvement.

The best model developed and proposed in this study performs well. However, to verify whether the model has overfitting problems, this study evaluates the model based on statistical indicators and physical meanings. First, by comparing the errors between the predicted values and the actual values in the test set, the difference between the two is small, indicating that the model has good generalization ability. In addition, the model is analyzed using quantitative evaluation indicators, and the results show that the model performs consistently in various statistical indicators, and there is no significant sign of increased verification error.

To further reduce the risk of overfitting, the a_{20} index is introduced into the model to analyze and control the model from the physical meaning. The specific prediction table is shown in Appendix A. From the data

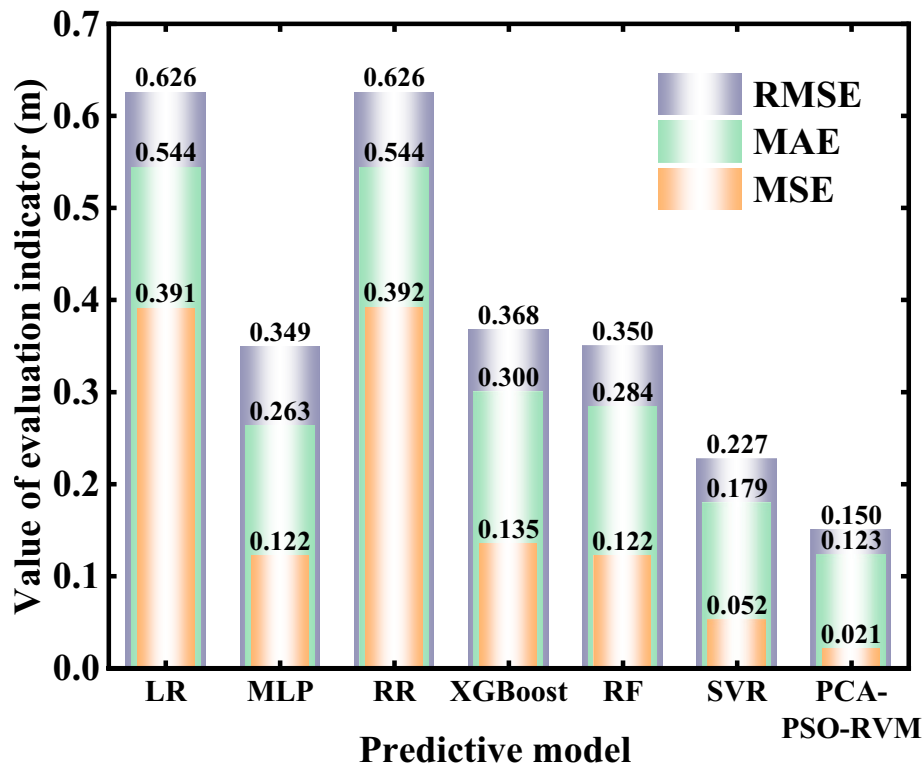


Fig. 14 RMSE, MAE and MSE evaluation indicators for each model

in the table, it can be seen that a_{20} of the collaborative optimization model is 1, indicating that the prediction effect of the model is good and the reliability is strong. These measures effectively prevent overfitting problems, improve the model's predictive ability on unknown data, and ensure the robustness and reliability of the proposed model.

4.4 Limitations and Future Research

The collaborative optimization model proposed in this study performs well in SCC strength prediction. However, it is difficult to interpret due to high quality and data dependence. It is difficult to intuitively understand which features have an important impact on the prediction, which limits its application in practical engineering. In the future, the generalization ability and training efficiency of the model can be improved using data enhancement technology. Develop a more interpretable and visualization-friendly model to enhance the acceptability of the model in practical engineering.

5 Conclusion

In this study, based on the PCA-PSO-RVM model to predict the strength of SCC, the main conclusions are as follows:

- 1. This study addresses the issues of multi-parameter coupling effects and insufficient prediction accuracy of traditional empirical models in the compressive strength prediction of SCC by proposing a hybrid machine learning prediction model based on PCA, PSO, and RVM. The model employs PCA for feature extraction and dimensionality reduction of raw material parameters, effectively resolving the redundancy problem of high-dimensional data. It also utilizes the PSO algorithm to optimize the hyperparameters of the RVM model, significantly enhancing prediction performance. The results demonstrate that this approach offers a novel technical solution for the compressive strength prediction of SCC, with important theoretical and practical engineering implications.
- 2. Compared with traditional models, such as linear regression, MLP, ridge regression, XGBoost, random forest regressor, and SVR, the proposed PCA-PSO-RVM model shows superiority in all evaluation indices. Specifically, the PCA-PSO-RVM model achieves 33.92%, 59.61%, and 31.28% reductions in RMSE, MSE, and MAE, respectively, while its R² improves by 5.16%, compared to the suboptimal SVR model. This result fully confirms the significant advantages of the PCA-PSO-RVM model in terms

- of prediction accuracy, error dispersion, and model generalization ability.
- 3. The SCC strength prediction model based on PCA-PSO-RVM effectively solves the problem of insufficient prediction accuracy of traditional methods under the influence of multi-factor coupling, which is of great value to improve the quality, safety, economic benefits, and environmental protection of engineering. Future research can integrate multi-source data, enhance the model interpretability, expand the scope of engineering applications, and quantify the prediction uncertainty to improve the generalization ability, prediction accuracy, and engineering practicability of the model, and to provide a more powerful tool for the performance evaluation and optimal design of SCC.

Appendix A

No.	Actual value	Predictive value	P/A	Deviation within ±20%
71	1.362489553	1.3625	1.0000	Yes
72	0.326421665	0.3264	1.0001	Yes
73	-0.668728489	-0.6687	1.0000	Yes
74	0.911622454	0.9116	1.0000	Yes
75	1.208855045	1.2089	1.0000	Yes
76	0.314841175	0.3148	1.0001	Yes
77	-0.647883606	-0.6479	1.0000	Yes
78	-1.428408668	-1.4284	1.0000	Yes
79	0.899269931	0.8993	1.0000	Yes
80	0.158118536	0.1581	1.0001	Yes
81	0.257710755	0.2577	1.0000	Yes
82	-0.860192599	-0.8602	1.0000	Yes
83	1.45590551	1.4559	1.0000	Yes
84	1.282198152	1.2822	1.0000	Yes
85	1.052132406	1.0521	1.0000	Yes
86	0.444542669	0.4445	1.0001	Yes
87	-1.323412221	-1.3234	1.0000	Yes
88	-1.379770608	-1.3798	1.0000	Yes
89	-1.385174837	-1.3852	1.0000	Yes
90	-1.346573202	-1.3466	1.0000	Yes
91	0.622110191	0.6221	1.0000	Yes
92	0.251534493	0.2515	1.0001	Yes
93	0.413661361	0.4137	0.9999	Yes
94	-0.554467649	-0.5545	0.9999	Yes
95	0.203668466	0.2037	0.9998	Yes
96	1.458221608	1.4582	1.0000	Yes

No.	Actual value	Predictive value	P/A	Deviation within ±20%
97	-1.326500352	-1.3265	1.0000	Yes
98	0.433734211	0.4337	1.0001	Yes
99	-1.34039694	-1.3404	1.0000	Yes

Abbreviations

PCA	Principal component analysis
PSO	Particle swarm optimization
RVM	Relevance vector machine
SCC	Self-compacting concrete
ELM	Extreme learning machine
ANFIS	Adaptive fuzzy neural inference system
MARS	Multiple adaptive regression splines
XGBoost	Extreme gradient boosting
SVM/SVR	Support vector machine/support vector machine regression
MLP	Multilayer perceptron regression
KMO	Kaiser-Meyer-Olkin

cinal camananant analysis

Acknowledgements

The authors thank the financial support provided by National Natural Science Foundation of China under Grant No.52068016. The work in this study was also supported by the Guangxi Key Laboratory of Geomechanics and Geotechnical Engineering (Grant No.20-Y-XT-01).

Author contributions

YZ: conceptualization, methodology, and funding acquisition; YLY: writing—original draft and editing, data curation, and formal analysis; JFW: validation, software, methodology, and data curation; BCT: visualization, investigation, software, and investigation; FF: project administration, supervision, and writing—review and editing.

Funding

The National Natural Science Foundation of China (Grant No.52068016), Guangxi Key Laboratory of Geomechanics and Geotechnical Engineering (Grant No.20-Y-XT-01).

Available of data and materials

The data supporting the findings of this study are available within the article. The models or code generated or used during the study are available from the corresponding author by request.

Declarations

Ethics Approval and Consent to Participate

All authors of the manuscript confirm ethical approval and consent to participate following the Journal's policies.

Consent for Publication

All authors of the manuscript agree on the publication of this work in the International Journal of Concrete Structures and Materials.

Competing Interests

The authors declare that they have no known competing financial interests or personal relationships that could have appeared to influence the work reported in this paper.

Received: 20 December 2024 Accepted: 30 July 2025 Published online: 24 October 2025

References

- Adhikary, S. K., Ashish, D. K., Sharma, H., Patel, J., Rudžionis, Ž, Al-Ajamee, M., Thomas, B. S., & Khatib, J. M. (2022). Lightweight self-compacting concrete: A review. Resources, Conservation & Recycling Advances., 15, 2667–3789. https://doi.org/10.1016/j.rcradv.2022.200107
- Akande, K., Owolabi, T., Twaha, S., & Olatunji, S. (2014). Performance comparison of svm and ann in predicting compressive strength of concrete. IOSR Journal of Computer Engineering, 16, 88–94. https://doi.org/10.9790/0661-16518894
- Apostolopoulou, M., Asteris, P., Armaghani, D. J., Douvika, M., Lourenco, P., Cavaleri, L., Bakolas, A., & Moropoulou, A. (2020). Mapping and holistic design of natural hydraulic lime mortars. *Cement and Concrete Research*. https://doi.org/10.1016/j.cemconres.2020.106167
- Armaghani, D. J., & Asteris, P. G. (2021). A comparative study of ANN and ANFIS models for the prediction of cement-based mortar materials compressive strength. *Neural Computing & Applications*, 33(9), 4501–4532. https://doi.org/10.1007/s00521-020-05244-4
- Asteris, P. G., & Kolovos, K. G. (2019). Self-compacting concrete strength prediction using surrogate models. *Neural Computation & Applications, 31*(1), 409–424. https://doi.org/10.1007/s00521-017-3007-7
- Asteris, P., Kolovos, K., Douvika, M., & Roinos, K. (2016). Prediction of selfcompacting concrete strength using artificial neural networks. *European Journal of Environmental and Civil Engineering*. https://doi.org/10.1080/ 19648189.2016.1246693
- Asteris, P., Karoglou, M., Skentou, A., Vasconcelos, G., He, M., Bakolas, A., Zhou, J., & Armaghani, D. J. (2024). Predicting uniaxial compressive strength of rocks using ann models: Incorporating porosity, compressional wave velocity, and Schmidt hammer data. *Ultrasonics*. https://doi.org/10.1016/j.ultras.2024.107347
- Banfill, P. F. G., Teixeira, M. A. O. M., & Craik, R. J. M. (2011). Rheology and vibration of fresh concrete: Predicting the radius of action of poker vibrators from wave propagation. *Cement and Concrete Research*, *41*(9), 932–941. https://doi.org/10.1016/j.cemconres.2011.04.011
- Ding, X., Li, C., Li, Y., Lu, Y., Song, C., & Zhao, S. (2018). Experimental and numerical study on stress-strain behavior of self-compacting SFRC under uniaxial compression. *Construction and Building Materials*, 185, 30–38. https://doi.org/10.1016/j.conbuildmat.2018.07.020
- Domone, P. L. (2007). A review of the hardened mechanical properties of self-compacting concrete. *Cement and Concrete Composites*, *29*(1), 1–12. https://doi.org/10.1016/j.cemconcomp.2006.07.010
- Douglas, H. R. (2019). Future directions for design, specification, testing, and construction of durable concrete structures. *Cement and Concrete Research*, 124, 105827. https://doi.org/10.1016/j.cemconres.2019.105827
- Dutta, S., Murthy, A., Kim, D., & Samui, P. (2017). Prediction of compressive strength of self-compacting concrete using intelligent computational modeling. Computers. Mater. Con., 53, 167–185. https://doi.org/10.1016/j. matpr.2022.02.487
- Gui, H., Xiang, J., Xing, T., Liu, J., Chu, Z., He, X., & Liu, C. (2022). Boundary element method with particle swarm optimization for solving potential problems. *Advanced Engineering Software*, 172, 103191. https://doi.org/10.1016/j.advengsoft.2022.103191
- Hooton, R. D., & Bickley, J. A. (2014). Design for durability: The key to improving concrete sustainability. *Construction and Building Materials*, *67*, 422–430. https://doi.org/10.1016/j.conbuildmat.2013.12.016
- Huang, L., Asteris, P. G., Koopialipoor, M., Armaghani, D. J., & Tahir, M. M. (2019). Invasive weed optimization technique-based ann to the prediction of rock tensile strength. *Applied Sciences*, 9(24), 5372. https://doi.org/10. 3390/app9245372
- Jahed, A. D., Mamou, A., Maraveas, C., Roussis, P., Siorikis, V., Skentou, A., & Asteris, P. (2021). Predicting the unconfined compressive strength of granite using only two non-destructive test indexes. *Geomech. Eng.*, 25, 317–330. https://doi.org/10.12989/gae.2021.25.4.317
- Kennedy, J., and R. Eberhart, 1995. "Particle swarm optimization." Proceedings of ICNN'95 - International Conference on Neural Networks 4, 1942-1948 https://doi.org/10.1109/ICNN.1995.488968.
- Koch, J. A., Castaneda, D. I., Ewoldt, R. H., & Lange, D. A. (2019). Vibration of fresh concrete understood through the paradigm of granular physics. *Cement and Concrete Research*, *115*, 31–42. https://doi.org/10.1016/j.cemconres. 2018.09.005

- Lee, L. (2021). On overview of PCA application strategy in processing high dimensionality forensic data. *Microchemical Journal, 169*, 106608. https://doi.org/10.1016/j.microc.2021.106608
- Li, J., Tan, D., Zhang, X., Wan, C., & Xue, G. (2021). Mixture design method of self-compacting lightweight aggregate concrete based on rheological property and strength of mortar. *Journal of Building Engineering*, 43, 102660. https://doi.org/10.1016/j.jobe.2021.102660
- Mai, H. V. T., Nguyen, T. A., Ly, H. B., & Tran, V. Q. (2021). Prediction compressive strength of concrete containing ggbfs using random forest model. *Acta Geotechnica*, 2021, 6671448. https://doi.org/10.1155/2021/6671448
- Saha, P., Prasad, M. L. V., & Kumar, P. R. (2017). Predicting strength of scc using artificial neural network and multivariable regression analysis. Computers and Concrete, 20(1), 31-38. https://doi.org/10.12989/cac.2017.20.1.031.
- Mrówczyńska, M., Sztubecki, J., & Greinert, A. (2020). Compression of results of geodetic displacement measurements using the PCA method and neural networks. *Measurement*, 158, 107693. https://doi.org/10.1016/j.measurement.2020.107693
- Okamura, H., & Ouchi, M. (1998). Self-compacting high performance concrete. Engineering and Materials, 1(4), 378–383. https://doi.org/10.1002/pse. 2260010406
- Rajakarunakaran, S., Lourdu, A., Muthusamy, S., Panchal, H., Jawad Alrubaie, A., Jaber, M., Ali, M., Tlili, I., Maseleno, A., Majdi, A., & Masthan Ali, S. H. (2022). Prediction of strength and analysis in self-compacting concrete using machine learning based regression techniques. Advanced Engineering Software, 173, 103267. https://doi.org/10.1016/j.advengsoft.2022.103267
- Sabet, F. A., Libre, N. A., & Shekarchi, M. (2013). Mechanical and durability properties of self consolidating high performance concrete incorporating natural zeolite, silica fume and fly ash. *Construction and Building Materials*, 44, 175–184. https://doi.org/10.1016/j.conbuildmat.2013.02.069
- Shami, T. M., El-Saleh, A. A., Alswaitti, M., Al-Tashi, Q., Summakieh, M. A., & Mirjalili, S. (2022). Particle swarm optimization: A comprehensive survey. *IEEE Access*, 10, 10031–10061. https://doi.org/10.1109/ACCESS.2022.3142859
- Siddique, R., Aggarwal, P., & Aggarwal, Y. (2011). Prediction of compressive strength of self-compacting concrete containing bottom ash using artificial neural networks. *Advanced Engineering Software, 42,* 780–786. https://doi.org/10.1016/j.advengsoft.2011.05.016
- Skentou, A. D., Bardhan, A., Mamou, A., Lemonis, M. E., Kumar, G., Samui, P., Armaghani, D. J., & Asteris, P. G. (2023). Closed-form equation for estimating unconfined compressive strength of granite from three non-destructive tests using soft computing models. *Rock Mechanics and Rock Engineering*, 56(1), 487–514. https://doi.org/10.1007/s00603-022-03046-9
- Smola, A. J., & Schölkopf, B. (2004). A tutorial on support vector regression. Statistics and Computing, 14(3), 199–222. https://doi.org/10.1023/B:STCO. 0000035301.49549.88
- Su, C., Liu, C., Jiang, S., & Wang, Y. (2021). Probabilistic power flow for multiple wind farms based on RVM and holomorphic embedding method. *Inter*national Journal of Electrical Power, 130, 106843. https://doi.org/10.1016/j. ijepes.2021.106843
- Susilorini, R. M. I. R., Iskandar, I., & Santosa, B. (2022). Long-term durability of bio-polymer modified concrete in tidal flooding prone area: A challenge of sustainable concrete materials. *Sustainability*, *14*(3), 1565. https://doi.org/10.3390/su14031565
- Tian, Z., Sun, X., Su, W., Li, D., Yang, B., Bian, C., & Wu, J. (2019). Development of real-time visual monitoring system for vibration effects on fresh concrete. *Automation in Construction*, 98, 61–71. https://doi.org/10.1016/j.autcon. 2018.11.025
- Tipping, M. E. (2001). Sparse bayesian learning and the relevance vector machine. *Journal of Machine Learning Research*, 1, 211–244. https://doi.org/10.1162/15324430152748236
- Tran, V. Q., Mai, H. V. T., Nguyen, T. A., & Ly, H. B. (2022). Assessment of different machine learning techniques in predicting the compressive strength of self-compacting concrete. *Frontiers in Structural and Civil Engineering*, 16(7), 928–945. https://doi.org/10.1007/s11709-022-0837-x
- Wang, X., Jiang, B., & Lu, N. (2018). Adaptive relevant vector machine based rul prediction under uncertain conditions. ISA Transactions. https://doi.org/ 10.1016/j.isatra.2018.11.024
- Wu, Y., & Li, S. (2022). Damage degree evaluation of masonry using optimized SVM-based acoustic emission monitoring and rate process theory. *Measurement*, 190, 110729. https://doi.org/10.1016/j.measurement.2022. 110729

- Xing, Z., Zhu, J., Zhang, Z., Qin, Y., & Jia, L. (2022). Energy consumption optimization of tramway operation based on improved PSO algorithm. *Energy*, 258, 124848. https://doi.org/10.1016/j.energy.2022.124848
- Yu, Y., Li, Y., Zeng, D., Hu, Y., & Yang, J. (2024). Permanent magnet synchronous motor demagnetization fault diagnosis based on PCA-ISSA-PNN. *Scientific Reports*, 14(1), 21921. https://doi.org/10.1038/s41598-024-72596-5
- Zadeh, A., Zafari, B., & Yaminpour, M. (2014). Multifunctional use of self-compacting concrete as a fundamental material in dam construction: Upper gotvand dam. *Key Engineering Materials*, 629–630, 391–398. https://doi.org/10.4028/www.scientific.net/KEM.629-630.391
- Zeng, Z., Huang, X., Yan, B., Wang, W., Ahmed Shuaibu, A., & He, X. (2021).

 Research on the fatigue performance of self-compacting concrete structure in CRTSIII slab ballastless track under the action of heavy haul train.

 Construction and Building Materials, 303, 124465. https://doi.org/10.1016/j.conbuildmat.2021.124465
- Zhang, C., Sun, Y., Xu, J., & Wang, B. (2021). The effect of vibration mixing on the mechanical properties of steel fiber concrete with different mix ratios. *Materials*, 14(13), 3669. https://doi.org/10.3390/ma14133669
- Zhang, P., Dongsheng, S., Ping, H., & Z. (2024). Study on the mechanical properties and pore structure of granulated blast furnace slag self-compacting concrete based on grey correlation theory. *Journal of Asian Architecture and Building Engineering*, 23(2), 634–648. https://doi.org/10.1080/13467581.2023.2244559
- Zoremsanga, C., & Hussain, J. (2024). Particle swarm optimized deep learning models for rainfall prediction: A case study in Aizawl, Mizoram. *IEEE Access*, 12, 57172–57184. https://doi.org/10.1109/ACCESS.2024.3390781

Publisher's Note

Springer Nature remains neutral with regard to jurisdictional claims in published maps and institutional affiliations.

Yan Zhang PhD,Professor, Gruangxi Key Laboratory of Geomechanics and Geotechnical Engineering, Guilin Universty of Technology, Guilin,541004,China

Yulong Ye Master, College of Civil and Architectural Engineering, Guilin University of Technology, Guilin, 541004, China

Junfeng Wang Master, College of Civil and Architectural Engineering, Guilin University of Technology, Guilin, 541004, China

Beichang Tang Master, College of Civil and Architectural Engineering, Guilin University of Technology, Guilin, 541004, China

Feng Fu PhD, Associate Professor Department of Engineering, School of Science & Technology, City, University London, Northamp-ton Square, London, UK, EC1VOHB: Adjunct Professor, College of Civil and Architectural Engineering, Guilin University of Technology, China, 541004